Proceedings of ITC18,2008

Conceptual Design and Development of an Indirect-cooled Superconducting Helical Coil in FFHR

Hitoshi Tamura, Kazuya Takahata, Toshiyuki Mito, Shinsaku Imagawa, Akio Sagara

National Institute for Fusion Science, 322-6 Oroshi-cho, Toki, Gifu 509-5292, Japan

FFHR is the name for a conceptual design of a heliotron fusion reactor being developed at the National Institute for Fusion Science. All the coils in the FFHR are made of superconductors. Several cooling schemes have been proposed for the helical coils and indirect cooling is considered a good candidate. In this study, we investigated the possibility of using an indirect-cooled superconducting magnet for the FFHR. In parallel with this design study, we developed the Nb_3Sn superconductor, jacketed with an aluminum alloy, for use in an indirect-cooled magnet. The results of performance tests for a sub-scale superconductor showed good feasibility for application in the FFHR helical coil. Stress distribution in the helical coil was also analyzed, and the stress and strain were confirmed to be within the permissible range.

Keywords: large helical device, helical reactor, indirect-cooled superconducting magnet, Nb_3Sn superconductor, cable-in-conduit-conductor, stress analysis

1. Introduction

Experimental results of the large helical device (LHD) have revealed that an LHD-type helical reactor is well suited as a demonstration device of a fusion power plant [1]. FFHR is the name for the conceptual design of an LHD-type heliotron fusion reactor. The magnet system of the FFHR includes one pair of superconducting helical coils and two pairs of superconducting poloidal coils. Several cooling schemes have been proposed for these superconducting helical coils—forced-flow and indirect cooling are considered good candidates. The former with a cable-in-conduit conductor (CICC) has been chosen for designs of many large-scale experimental fusion magnets, such as the poloidal coils of the LHD, the main coils of ITER, Wendelstein 7-X, and JT-60SA, because of its mechanical strength and electrical/thermal stability. On the other hand, indirect cooling solves the problem of pressure drops in the CICC. Furthermore, a superconducting magnet with indirect cooling is considered to have better mechanical rigidity, since its structural components, such as the superconducting strands, cabling jacket, insulators, cooling panels, and coil case, are completely in contact with each other.

In this study, we investigated the possibility of using an indirect-cooled superconducting magnet for the FFHR. In parallel with this study, we developed Nb_3Sn superconductors, jacketed with an aluminum alloy, for use in the indirect-cooled magnet. The "react-and-wind" process can be performed on a large superconducting coil using this type of superconductor, since the jacketing can be performed after heat treatment of the superconducting strands by friction stir welding (FSW). The development details of sample conductors and the results of performance tests for the sub-scale superconductor are also shown.

author's e-mail: tamura@nifs.ac.jp

2. Structure of the Coil

Fig. 1 shows a schematic of the cryogenic components in the FFHR. The major and minor radii of the helical coils are approximately 14–16 and 4 m, respectively. The total magnet energy of the coils is 120 GJ. The electromagnetic force generated by these coils is sustained by inner and outer supporting structures. The magnetic field at the plasma center is 6.18 T. The cross sectional dimension of the helical coil was determined by considering the geometry of the plasma facing components. Fig. 2 shows a conceptual design of the cross section of the helical coil. It has a rectangular cross-section, 1.8 m in width and 0.9 m in height. There were 432

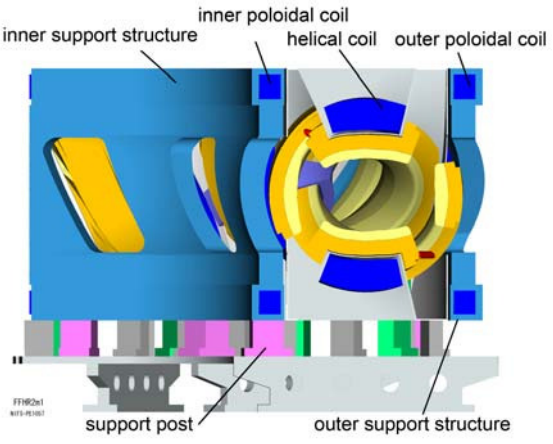

Fig.1 Schematic of the cryogenic components in the FFHR.

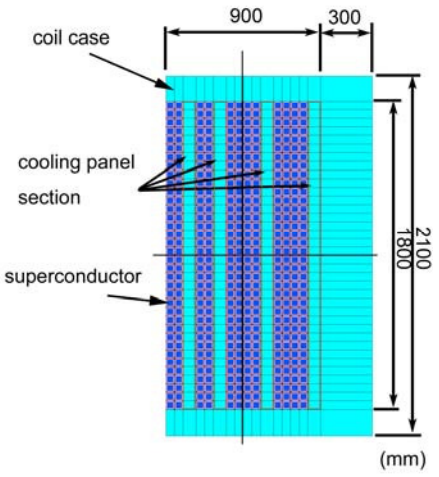

Fig. 2 Cross-sectional view of the conceptual design of the indirect-cooled helical coil.

superconductors (36 turns, 12 layers) made of Nb_3Sn and a jacketing material. An aluminum alloy was chosen as the jacketing material, because it offers high thermal conductivity and mechanical strength. The cooling panels were placed at every two or four turns of the winding. Each cooling panel is 75 mm thick and the superconductor is indirectly cooled by this cooling panel. The coil is wound along the coil case made of stainless steel (SS) and covered with a lid. The LHD-type helical reactor does not require plasma current so there is little AC loss in the magnet. The heat load to the coil during reactor operation comes mainly from nuclear heating. Takahata et al. calculated the elimination of this steady state heat load and showed that an aluminum jacket superconductor with a cooling panel could resolve this issue [4].

3. Development of the Aluminum Alloy Jacketed Superconductor

3.1 Specification and fabrication process

The fundamental geometry of the superconductor is a 50 mm square shape, including insulation. Since the maximum magnetic field at the coil region is around 13 T, Nb_3Sn wires can be used. The operating current is 100 kA and the overall current density is 40 A/mm^2. Since the melting point of aluminum alloy (933 K) is lower than that of the heat treatment temperature of the Nb_3Sn wires (1000 K), the jacketing must be performed after the heat treatment of the wires. We developed a conductor fabrication process, using a FSW technique that uses friction heating, to avoid the temperature rise in the welding region. The superconducting wire is embedded in the aluminum alloy jacket with a solder material and the lid is welded by the FSW. The solder can be automatically melted and it fills the void around the superconducting

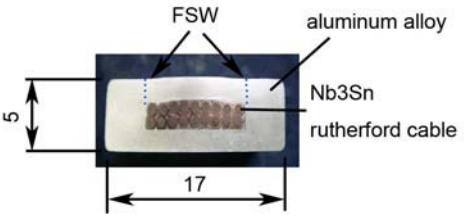

Fig. 3 Photo of the cross-section of reduced size 4.7 kA class sample superconductor.

wire. A prototype 10 kA class superconductor with 17 mm square shape was made to demonstrate the fabrication process and the performance of the conductor. It showed 19 kA transport current at 8 T and confirmed that although there was some degradation in the critical current, it was not due to the fabrication process, but the difference in thermal contraction between Nb_3Sn and aluminum alloy [4].

3.2 Reduced size sample test

To confirm the allowable bending deformation, 4 kA class superconductors, made of Nb_3Sn cable and aluminum alloy jackets using the same production process as the previous 10 kA class sample, were manufactured. The packing factor of the superconductor inside the aluminum jacket was increased from 60% to 80%. Fig. 3 shows the cross-sectional structure of the sample conductor and its dimensions. The following two samples were tested: (1) without bending, and (2) bent once along a rig, with a radius of 150 mm then bent back to the original straight shape (R150S). Fig. 4 shows the experimental results of current-carrying capacity tests. The open plot indicates the critical currents (definition; 1 μV/cm) of the test conductor at 4.4 K and the error bars represent the maximum and

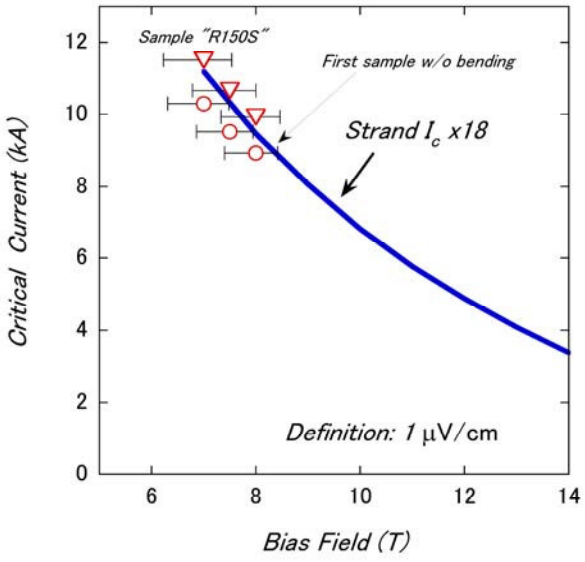

Fig. 4 Critical currents of the reduced size superconductor, with and without bending.

minimum magnetic field inside the conductor. The solid line indicates the critical current of the strand, multiplied by 18 (the number of strands). We succeeded in carrying a current of 11 kA at 8 T with the sample R150S. This confirms that the critical current was not affected by bending. Furthermore, the critical current of sample R150S might be increased by the pre-bending effect [5].

4. Comparison with CICC

Here we simply compared the apparent rigidity between the indirect-cooled and CICC type superconductors. Fig. 5 shows models of the superconductors. The indirect-cooled superconductor has a 50 mm square shape and a 32 mm square Nb_3Sn superconducting region filled with solder. The ratio of the superconductor to the solder is 8:2. The superconductor includes an 18-mm-thick aluminum alloy (6061 T6) and 1-mm-thick insulation. The CICC type has 90 kA of operating current with 480 superconductors made of Nb_3Sn. The conduit is 1.6 mm thick and the conductor is embedded in the internal plate. Both components are made of SS. There is an insulator between the conduit and the internal plate.

The longitudinal rigidity was estimated according to the rule of mixture, using the area fraction of each structural component. The cross-sectional rigidity was calculated by modeling each conductor type with the finite element method (FEM) model. In this case, the plane strain model was adopted, and the rigidity was calculated from the result of reaction force against the force displacement at the top of the conductor. In the indirect-cooled type, the material properties of the superconducting region were selected according to the rule of mixture. On the other hand, in the superconducting region in the CICC type it was assumed that it did not contribute to the mechanical rigidity of the cross-sectional direction. The other components were treated as isotropic materials. The material properties of the components at a cryogenic temperature (4 K) [6-8] were used in the analytical model. The material properties used in the calculation are shown in Table 1.

The longitudinal rigidity of indirect-cooled and CICC superconductors were estimated at 82 and 109 GPa, respectively. The former coil has a cooling panel, which also contributes to coil rigidity. If the cooling panel has a longitudinal rigidity of 163 GPa, the indirect-cooled coil can provide reasonable overall rigidity compared with the CICC coil. Assuming that the cooling panel consists of a SS case and a cooling mechanism, 20% of the cooling panel area can be used for the mechanism. The cross-sectional rigidity of the indirect-cooled and CICC types were 79 and 56 GPa, respectively.

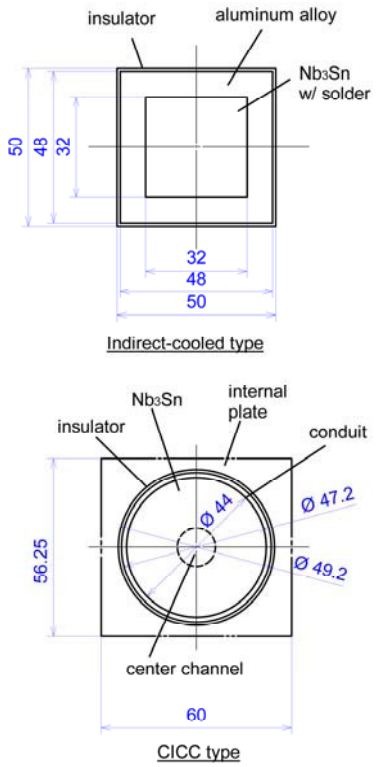

Fig. 5 Rigidity evaluation model for the indirect -cooled (upper) and CICC (lower) superconductors.

Table 1. Material property of components.

	Young's modulus (GPa)	Poisson's ratio	note
Nb_3Sn	100	0.3	
Aluminum	77	0.327	6061-T6
Insulator	80	0.3	Alumina w/ epoxy
Stainless steel	208	0.284	SS316
Solder	40	0.3	Pb free

5. Coil rigidity evaluation

5.1 Analytical model

The helical coil of the FFHR has a three-dimensional structure, with a change in its curvature in the toroidal angle. It is believed that a circular coil with an average curvature similar to that of an actual helical coil can estimate the mechanical behavior of the coil [9]. We calculated the stress and strain distribution inside the coil to confirm the stress and strain levels. The average radius of curvature of the helical coil was 5.5 m at the center of the cross section of the coil. The cross-sectional structure of the helical coil, shown in fig. 2, was used to create the FEM model. The radius from the central axis to the center of the coil cross section was set at the average of the curvature of the helical coil. The insulator used in the superconductors was assumed to be made of alumina

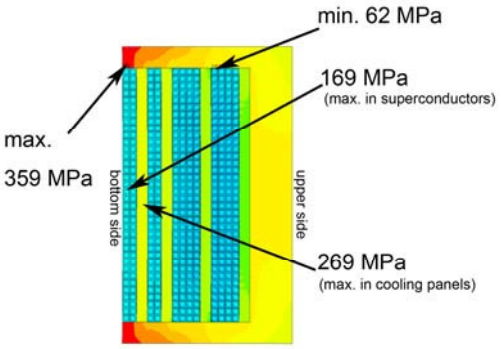

Fig. 6 Hoop stress distribution by the radial electromagnetic force.

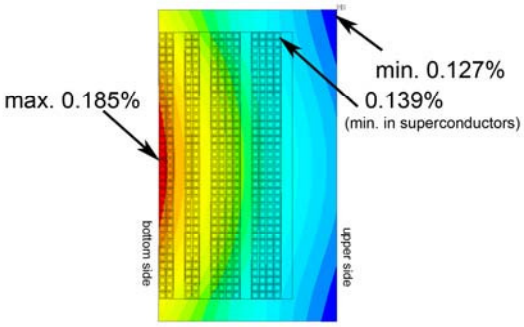

Fig. 7 Circumferential strain distribution by the radial electromagnetic force.

ceramics and resin. The SS coil case, with a thickness of 300 mm at the top and 150 mm on both sides of the coil section, was used.

An electromagnetic force was applied as the body force by multiplying the current density and the magnetic field in every single superconducting region to ensure that the electromagnetic force was precisely applied to the coil. The electromagnetic force considered here was in the radial direction of the circular coil since it generated the hoop force inside the coil. The hoop force is more effective for the superconductor than the overturning force at a point of strength of the coil structure. Although the magnetic field intensity was different at every cross section, an averaged magnetic field was applied at every single superconducting position along the circumference. Furthermore, a constant value was added to the averaged magnetic field so that the total hoop force in the cross section was equal to the maximum overall hoop force. ANSYS version 11.0 was used, and the three-dimensional axisymmetric solid element was adopted.

5.2 Result

The material properties were set using the values described in section 4. It was assumed that the cooling panel had 80% of Young's modulus for SS316. Figs. 6,7 show the results of the hoop force analysis with respect to the hoop stress distribution, the hoop strain distribution, and the radial displacement distribution, respectively. The maximum hoop stress of 359 MPa appeared in the side wall of the coil case. In the coil winding section and the cooling panel section, the maximum stress was 169 and 269 MPa, respectively. The strain from hoop force was 0.185% at the bottom center of the superconductor. The components in the coil were subjected to compressive stress towards the coil center region. All stress and strain levels for each component were within the permissible values.

6. Conclusions

In conceptual design studies of the FFHR, indirect-cooled superconducting helical coils have been proposed. The aluminum-alloy-jacketed Nb_3Sn superconductors with a cooling panel can prove the feasibility of this approach. The following results were obtained in this study: (1) A reduced sample size of the aluminum-alloy-jacketed Nb_3Sn superconductor showed good performance and the critical current did not degrade by bending. (2) The cooling panel requires a longitudinal rigidity of 163 GPa to provide same rigidity as a helical coil using CICC. (3) The indirect-cooled type superconductor has much higher cross-sectional rigidity than the CICC. (4) Stress and strain distributions in the indirect-cooled helical coil, investigated by the FEM model, were confirmed to be within the permissible range.

Acknowledgments

The authors wish to express their thanks to Mr. M. Sugimoto of the Furukawa Electric Co., Ltd. for his efforts in developing a superconductor for the candidate system. This work was supported by the National Institute for Fusion Science (08ULAA107, 08ULAA117).

References

[1] O. Motojima *et al*., Fusion Eng. Des. **81** 2277 (2006).
[2] A. Sagara *et al*., Nucl. Fusion **45** 258 (2005).
[3] A. Sagara *et al*., Fusion Eng. Des. **81** 2703 (2006).
[4] K. Takahata *et al*., Fusion Eng. Des. **82** 1487 (2007).
[5] G. Nishijima *et al*., IEEE. Trans. Appl. Supercond. **16** 1220 (2006).
[6] Cryocomp software (Eckels Engineering and Cryodata Inc., 1997).
[7] D. Mann, *LNG Materials and Fluids* (National Bureau of Standards, 1977).
[8] N. Mitchell, Cryogenics **45** 501 (2005).
[9] H. Tamura *et al*., Journal of Physics: Conference Series **97** 012139 (2008).